Energetics, Dynamics, and Reactions of Rydberg State Molecules in van der Waals Clusters

Quan Yuan Shang† and Elliot R. Bernstein*

Department of Chemistry, Colorado State University, Fort Collins, Colorado 80523

Received January 27, 1994 (Revised Manuscript Received May 30, 1994)

Contents

I. Introduction 2015
II. Technical Advances for Probing Molecular Clusters 2016
A. Supersonic Jet 2016
B. Probe Techniques 2017
1. Absorption Spectroscopy 2017
2. Laser-Induced Fluorescence (LIF) 2017
3. Mass-Resolved Excitation Spectroscopy (MRES) 2017
4. Hole Burning/Population Depletion 2017
5. Nozzle/Laser Timing Delay 2017
6. Two-Color Ionization 2018
7. Ionization Action Spectrum 2018
8. Pump/Probe Ionization Lifetime 2018
C. Calculations 2018
III. Energetics of Rydberg State Solute/Solvent Interaction 2018
A. Repulsion—The Pauli Exclusion Principle 2018
1. Dioxane-, ABCO-, DABCO-, and HMT/Argon Clusters 2019
2. Clusters with Other Rare Gas Atoms 2021
3. Dioxane-, ABCO-, DABCO-, and HMT/Saturated Hydrocarbon Clusters 2021
4. Clusters with Other Solvents 2021
B. Attractive Dipole/Induced Dipole Interaction
C. Attractive Electron Transfer Interaction 2022
IV. Rydberg State Relaxation Dynamics and Reactions 2022
A. Intersystem Crossing 2022
B. Electron Transfer 2023
C. Energy Transfer 2024
V. Conclusions 2024

I. Introduction

In the past 10 years the study of van der Waals clusters has grown enormously;[1,2] perhaps one of the best indications of this growth, in both activity and sophistication, is the advent of this review issue devoted to such research. van der Waals clusters, synthesized one molecule or atom at a time and accessed according to size and structure, provide a molecule by molecule view of the solvation process, its energetics, solute/solvent dynamics, and eventually even unimolecular and bimolecular chemical reactions.[3-6] The clusters treated most frequently and discussed in this review are of the form solute or chromophore (solvent)$_n$, with n varying from 1 to more than 100. These clusters are most typically generated in a supersonic beam;[1-7] both large and small clusters can be synthesized by controlling the expansion conditions. For small clusters ($n \leq 10$), species with well-defined geometries and energies can thereby be obtained. Cluster energetics, structure, and dynamics can be probed spectroscopically (e.g., microwave, Raman, infrared, visible, ultraviolet, one photon, two photon, etc.) through states of the solute molecule or through intermolecular modes of the cluster.[1,2] The solute/solvent interaction (e.g., van der Waals, electrostatic, hydrogen bonding, charge transfer, etc.) can be elucidated through spectroscopic cluster shifts, defined as $[\nu(\text{cluster}) - \nu(\text{solute})] = \Delta\nu$. Energy dynamics and relaxation[7-10] (intracluster vibrational energy redistribution, IVR; vibrational predissociation, VP; intersystem crossing, ISC; etc.) and even chemical reactions can be directly probed in great detail for simple, well-designed, specifically constructed systems.[11] Careful sample preparation and access facilitate a direct comparison between experiment and theory. Thus, the study of clusters has become more than a science unto itself: it also provides insight into many condensed phase phenomena. A number of groups have employed cluster studies to elucidate solvent/solute energetics, structure and dynamics, and their work has been reviewed many times over the last 10 years.[1,2b,5]

A large number of van der Waals cluster studies have employed aromatic molecules as the solute species and $(\pi\pi^*) \leftarrow (\pi^2)$ or $(n\pi^*) \leftarrow (n^2)$ valence transitions as the electronic spectroscopic probe.[1a,b,2] These transitions are well-known and the behavior of valence transitions with regard to solvent perturbations is well documented. Quite recently advances have been made in the understanding of solvent effects and interactions for Rydberg transitions. Molecular Rydberg states are excited electronic states which are composed primarily of atomic orbitals with principal quantum numbers greater than that of the ground state and the valence excited states (e.g., $\pi\pi^*$, π^2, $n\pi$, etc.).[12] An electron in high-energy Rydberg orbital experiences the attractive potential of the central molecular ionic (+1) core and is well isolated from the valence states. Lower energy Rydberg orbitals (principal quantum number $n \sim 3, 4$) can, however, mix with similar energy valence orbitals. Nevertheless, this approximation provides a direct insight into the nature of the Rydberg orbital/solvent interaction. Since the Rydberg orbital is spatially extended and relatively removed from the ionic core, it is diffuse and highly polarizable. Such electronic

† Current address: Applied Materials, Santa Clara, CA 95054.

0009-2665/94/0794-2015$14.00/0

Quanyuan Shang was born in Jiangsu, China. He received his B. S. degree at Nanjing University. Through a Harvard CGP program, he went to the University of Oregon where he obtained his Ph.D. degree in Physical Chemistry in 1990 with Professor Bruce Hudson. He spent three years as a postdoctoral fellow with Professor Elliot Bernstein at Colorado State University. He is now a senior process engineer in Applied Komatsu Technology engaged in the development of plasma enhanced chemical vapor deposition equipment for flat panel displays. In his academic career, Dr. Shang's major research interest was in molecular electronic structures and chemical reactions in the excited electronic states. He has co-authored 16 publications. He discovered the transition dipole orientation of polyenes, pioneered the work of solvent perturbation on molecular Rydberg states in van der Waals clusters, and discovered and characterized electron-transfer reactions between molecular Rydberg states and polar solvents.

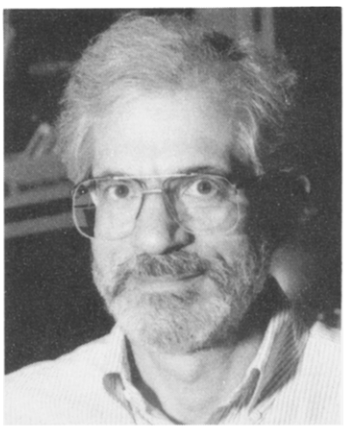

Elliot R. Bernstein was born in New York City, NY. He received his A.B. degree from Princeton University in 1963 and his Ph.D. degree from Caltech in 1967. As an undergraduate he did research with Donald F. Hornig and Walter Kauzmann. His Ph.D. studies were conducted under G. Wilse Robinson. He was a postdoctoral fellow with C. A. Hutchinson Jr. at the University of Chicago from 1967 to 1969. During this time he was a Natural Science Foundation Summer Fellow (1961, 1962), a Woodrow Wilson Fellow (1963, 1964), and an E. Fermi postdoctoral Fellow (1967 to 1969). After six years on the faculty of Princeton University, he joined the faculty at Colorado State University where he is currently Professor of Chemistry and Associate Chair of the Chemistry Department. Professor Bernstein is a member of the American Chemical Society and the American Association for the Advancement of Science, and a Fellow of the American Physical Society. He has over the years pursued a wide range of research interests including molecular crystal energy levels, energy transfer, and phase transitions; molecular and atomic liquid properties; isolated molecule structure, energy levels, and properties; the effect of solvation on isolated molecule properties and dynamics as elucidated through van der Waals complexes; and vibrational dynamics and predissociation in van der Waals complexes. Most recently he has turned his attention to two new areas: the properties of transient species (e.g., radicals, carbenes, nitrenes) and how they are affected by solvation in van der Waals complexes; and chemical reactions (e.g., electron transfer, proton transfer, radical addition, hydrogen abstraction, etc.) in van der Waals complexes.

states typically have a large polarizability: several hundred cubic angstroms for the (n3s) state of acetone, for example.[13]

Because an electron in a Rydberg orbital is only weakly bound to the ionic molecular core, a molecule in a Rydberg excited state can be quite reactive. Indeed, the formation of radicals and ions from Rydberg states requires typically less than 25 000 cm^{-1} and the cross section for ionization can be large. Rydberg excited molecules can thus play an important role as reactive intermediates in radiation, shock, and electrically initiated chemical reactions. Molecular photochemistry,[12,14] initial dissociation of energetic materials,[15] and astrochemistry[16] are areas for which the Rydberg states of molecules are of some concern and importance. Recent studies of ionic systems show the generality of these reactive election-transfer processes.[17]

The studies discussed in this review stem mostly from our efforts over the last three years. This work has led to some new insights into the basic electronic properties of Rydberg states and their chemical reactivity. Efforts of the few other groups in this area will also be mentioned as the current molecular Rydberg state story unfolds. In this review we will start with a discussion of techniques which have been developed over the last few years to deal specifically with reacting and fragmenting clusters in supersonically cooled cluster beams. This section will present static, spectroscopic, time-resolved approaches to the study of reacting, relaxing, dissociating, and evolving clusters and cluster vibronic states. Most of these approaches to the investigation of clusters are not necessarily developed for, or restricted to, the study of Rydberg states; in that sense, this review takes a more general approach, delineating the study of molecular clusters. In the next main section of this article we present a review of the energetics of Rydberg state/solvent interactions and a discussion of the decomposition of these interactions into a few types of limiting elementary forms. Following this, the dynamical and reaction behavior of Rydberg clusters is presented. Throughout this report emphasis is placed on general principles and systematics of Rydberg state/solvent interactions. Finally we summarize these studies and briefly discuss future efforts in this area of research.

II. Technical Advances for Probing Molecular Clusters

A. Supersonic Jet

Clusters of all sizes can be formed in the gas phase provided the molecules are present in sufficient concentration and the temperature is sufficiently low. One of the most valuable and enduring techniques of the last two decades has been the supersonic jet expansion. Cold molecules and clusters are formed as the expansion proceeds from high pressure, high temperature to low pressure, low temperature. The cooling follows the adiabatic (isentropic) expansion relation; translational temperatures can be as low as 0.01 K, rotational temperatures can be as low as 1

K, and vibrational temperatures can be ca. 10 K.[1] A number of detail treatments are readily available on this topic.[1,2b] Expansion gases can be He, Ne, Ar, and N_2 at 10−500 psi. Solute and solvent molecule concentrations range from 0.1 to 10% of the expansion gas. Enhanced cooling can arise from expansions with 10% Ar-, CH_4-, and CF_4/He mixtures, as well.

B. Probe Techniques

A number of techniques have been developed over the last 10 years or so to probe the electronic states of cold molecules and clusters generated in a supersonic expansion. In the next few paragraphs we present a survey of the various techniques employed to access and study cluster systems.

1. Absorption Spectroscopy

Standard optical absorption spectra can be obtained for molecules in a supersonic jet by employing conventional light sources and monochromators.[18] The main advantages of this spectroscopic approach include readily available light sources, broad tuning ranges (IR to VUV), and ease of data acquisition and analysis. The major disadvantage of this approach are low sensitivity and poor resolution; additionally, the composition of the beam cannot readily be determined in an absorption experiment.

2. Laser-Induced Fluorescence (LIF)

This spectroscopic technique is both sensitive and simple. A laser, with line width from 1 to 10^{-4} cm^{-1}, is employed to excite a molecular or cluster transition. If the species of interest absorbs a photon, it can emit one, and the emitted photons are detected either undispersed (fluorescence excitation) or dispersed (dispersed emission). Ground and excited electronic state energy levels (rotation and vibration) can be studied in this manner;[2b] many nonlinear, multiphoton, and time-resolved augmentations of this basic technique have been implemented.[1,19] Nonetheless, one still must rely on a detailed analysis of spectroscopic data to determine the nature and composition of the absorbing and emitting species.

3. Mass-Resolved Excitation Spectroscopy (MRES)

This approach to optical spectroscopy of molecules and clusters in a cold beam overcomes most of the problems and disadvantages of the techniques mentioned thus far. Two photons, often, but not necessarily, from different lasers, are employed to excite and detect the species of interest. The first absorbed photon creates the excited rovibronic state (as discussed above) and the second photon generates the molecular or cluster ion which is detected by a mass spectrometer (typically a time-of-flight system is most convenient).[1] The ions are created only if the first transition has occurred and thus by scanning the first laser (λ_1), as one would in a LIF experiment, and observing ion signal as a function of λ_1, a spectrum of a species of particular and predetermined mass is generated. This technique generates information on the excited electronic states of clusters of selected mass. Both one- and two-photon excitation spectra can be obtained in this manner. This approach has been particularly useful for the study of Rydberg states because they often lie at such high energies (greater than 50 000 cm^{-1}). Additionally, one- and two-photon selection rules are different and complementary, and two-photon transitions are laser polarization dependent. The intensity of a two-photon transition depends on the polarization of the photons: circular, linear parallel, or linear perpendicular polarizations of the protons cause different rovibronic transitions to occur.[19,20]

4. Hole Burning/Population Depletion

Often in the study of clusters one finds that a cluster of a specific mass can possess a number of different structures: that is, clusters can have different isomers. The technique of hole burning/population depletion has been developed to demonstrate this phenomenon.[21−23] The technique is complementary to MRES. A MRES is composed of features deriving from a cluster of a given mass: these features may include spectra due to chromophore internal modes, van der Waals cluster modes, and isomers. Identification of spectra due to clusters of different geometries but the same mass plays an important role in understanding the effect of solvation on the physical and chemical properties of the chromophore molecule. The hole burning/population depletion technique employs two lasers: the first laser (intense) drives or saturates the population of one cluster isomer species to the ion via a resonant intermediate transition. The one-color (1 + 1)- or (2 + 1)-MRES generated by the second laser will have a reduced signal for features associated with the saturated (depleted or "burned" population) species accessed by the first laser. In order to avoid detector saturation due to ions generated by the depleting first laser, the depletion laser beam is focused upstream (closer to the nozzle) from the extraction region of the mass spectrometer where the MRES detection laser is focused. Thus the spectroscopic probe laser interrogates a neutral molecular beam with a depleted population in a particular cluster size and geometry. For a 0.5 cm displacement in beam positions for these two lasers, the second laser is delayed in time by a few microseconds. This technique has been demonstrated in a number of instances to be a very powerful and useful one for cluster isomer identification.[21−23]

5. Nozzle/Laser Timing Delay

Pulsed nozzles are useful for supersonic jet/mass-detected molecular and cluster spectroscopy because they allow modest pumping speeds and capacities to be employed with the associated vacuum equipment. Because the pulsed nozzle has a finite opening and closing time, for a typical 100−150 μs gas pulse one might expect a 10−20 μs or more opening and closing time. We have found that the gas pulse has not reached an equilibrium distribution of species for at least this period of time. Thus one finds that the time at which a species signal maximum appears in a pulsed nozzle expansion depends on the expansion conditions, the species mass, and indeed even the species structure.[23,24] Larger clusters form later in

the expansion because they take more time (more collisions) to form and because they travel more slowly (beam velocity "slip").[2b] Thus, features appearing in a spectrum acquired in a given mass channel but arising from dissociation of higher mass clusters can be identified by noting their arrival time at the ionization region following pulsed nozzle opening. The time delay between nozzle and laser firing for a signal maximum of a given spectroscopic mass channel is directly related to the mass of the parent or nascent cluster formed in the expansion. Therefore one can characterize cluster size associated with a given feature in an MRES through the "arrival time" dependence of the signal following pulsed nozzle opening, even if the feature appears in a spectrum detected in a different mass channel.

6. Two-Color Ionization

Often (1 + 1)- or (2 + 1)-MRES can be accomplished by a single laser or color. The advantage of a single laser experiment is simplicity: temporal and spatial overlap need only be considered between the laser and the molecular beam. The disadvantages of the one-color experiment are cluster fragmentation due to excess energy in the cluster ion, inability to measure intermediate (resonant) state lifetime, and inability to determine ionization thresholds. These disadvantages can be overcome in a two-color experiment; typically a two-color experiment involves two separate, independently tuned and timed lasers. The concomitant increase in information on the sample is, however, an important part of the experimental investigation.[25]

7. Ionization Action Spectrum

Another advantage of a two-color MRES is that the ionization energy of the accessed species can be accurately determined through fixing the first transition energy (A ← X) and scanning the second (I_0 ← A). In this manner an ionization action spectrum can be obtained.[26] More sophisticated variants of this technique (ZEKE,[27] MATI,[28] field ionization of very high energy Rydberg state,[12b] etc.) can be employed to generate ground state vibrational spectra of the ion itself. This approach can even be employed to determine the nature of the intermediate state which can be different for isolated molecules and clusters especially as these states display dynamical behavior. Time evolution of the ionization action spectrum can be employed to determine both cluster dynamics and chemistry. Abrupt changes in the ionization action spectrum with cluster size and structure can be interpreted to suggest changes in cluster dynamics and chemistry.

8. Pump/Probe Ionization Lifetime

The ion signal intensity in a two-color MRES experiment can be measured as a function of time delay for the ionization pulse with respect to the excitation pulse. The loss of signal intensity as a function of delay time can be related to the intermediate excited state lifetime. The MRES-measured time dependence so obtained can often contain more information than the fluorescence decay time, if the nascent excited state evolves into new excited states that will not emit on the time scale of a typical beam experiment (ca. 10 μs). Such pump/probe experiments can identify triplet states,[29,30] electron-transfer states,[30] proton-transfer states,[31] cluster vibrational redistribution and predissociation,[9,10] internal conversion, and cluster energy transfer.[30] Dynamical behavior can be measured in this manner from subpicosecond to microsecond time scales.

C. Calculations

Spectroscopic studies of clusters cannot always provide complete elucidation of cluster structure.[1] Clusters can be large, can have many degrees of freedom, may not have a rigid structure, and their potential surfaces can have multiple minima. These multiple minima are often separated by only small internal barriers and rapid motion between these minima can be the rule rather than the exception.[1,32,33] The cluster potential surface is thereby not harmonic for the low energy motions. Calculations, both ab initio and semi-empirical, are of central importance to understanding cluster behavior. Theoretical calculation of the solute/solvent interaction energy,[1] potential energy surface as a function of electronic state of the solute,[2,32] and vibrational modes on this surface (harmonic and anharmonic)[32,34] can be used as an important guide to interpretation of experimental results. Two approaches can be taken to this effort. Ab initio calculations have been applied to small systems such as diatomic/rare gas clusters[35] and even larger clusters.[36,37] Empirical potential energy calculations employing exponential-six, Lennard-Jones, Morse, power series with Coulomb terms can also be usefully applied to understand and interpret many experiments on polyatomic solvents and larger clusters.[32,35,36] This latter approach follows along the lines laid down for macromolecular and crystal systems.[1] Clusters are in fact an excellent test system for such calculations and potential functions because they provide accurate and available detailed experimental data for comparison between results of calculations and experiments. Presently, crystal structure and free energy data are employed to set potential parameters for calculation of cluster properties; in the near future, perhaps cluster experimental results will be sufficient to refine parameters for calculation of condensed phase and macromolecular structure and dynamics.

III. Energetics of Rydberg State Solute/Solvent Interactions

A. Repulsion—The Pauli Exclusion Principle

Rydberg states are readily perturbed by their environment.[38] In the presence of an inert gas (e.g., N_2, rare gases, etc.) at medium pressures, the Rydberg transition experiences a blue shift and asymmetric broadening to higher energy. This phenomenon can be attributed to an exchange repulsion effect between the Rydberg electronic configuration of the "solute" and the closed shells of the solvent. In fact, this observation has become the empirical technique employed to distinguish Rydberg from valence states. Recent work from this laboratory,

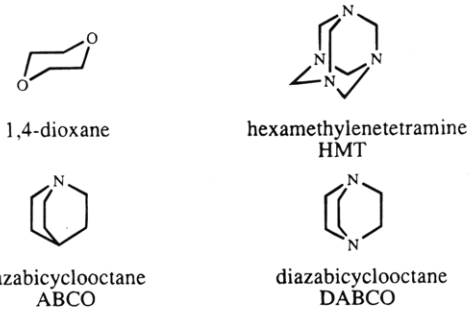

Figure 1. Molecular structures of 1,4-dioxane, hexamethylenetetramine (HMT), azabicyclooctane (ABCO), and 1,4-diazabicyclooctane (DABCO). The solvation effect on their (2p3s) Rydberg state will be presented in this review.

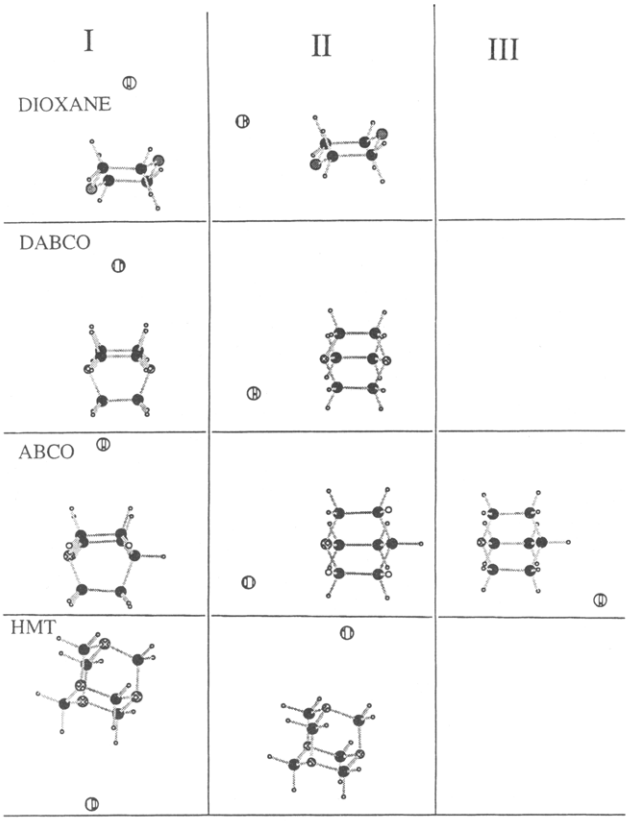

Figure 2. The calculated stable minimum energy geometries of dioxane$(Ar)_1$, DABCO$(Ar)_1$, ABCO$(Ar)_1$, and HMT$(Ar)_1$ employing a Lennard-Jones 6−12 van der Waals atom−atom potential. I, II, and III represent the three types of geometries calculated and assigned from spectra.

discussed below, on the Rydberg states of solute/solvent clusters gives a microscopic and detailed picture of these phenomena.

1. Dioxane-, ABCO-, DABCO-, and HMT/Argon Clusters

The (2p3s) ← $(2p)^2$ Rydberg transitions of cyclic ethers (1,4-dioxane,[39] Figure 1) and bi- and tricyclic amines (ABCO, DABCO,[23] HMT,[40] Figure 1) in argon clusters have been observed and analyzed with particular attention given to cluster transition energy shifts from the bare chromophore (solute) transitions. The solute/argon clusters in this instance can be expected to have a number of different geometries as indicated in Figure 2. Cluster structures are calculated with a Lennard-Jones 6−12 van der Waals potential[41] interaction for the ground electronic states of these species in the cluster. In all instances,

Table 1. The Binding Energy (BE) of Solute$(Ar)_1$ Cluster at Stable Minimum Energy Geometries in the Ground State[a]

	geometry I		geometry II		geometry III	
solute	BE	shift	BE[c]	shift	BE	shift
dioxane[b]	342	60	258	159	–	–
DABCO	341	105	293 (314)	290	–	–
ABCO	343	46	276 (300)	230	241	−28
HMT	289	51	308		–	–

[a] Calculated by employing a Lennard-Jones 6-12 interaction potential energy and (2p3s) transition energy shift with respect to the bare molecule (in cm^{-1}). See Figure 2 for the conformation of the cluster. [b] Argon parameters obtained to reproduce the $(Ar)_2$ binding energy (refs 23b and 41). [c] The number in parentheses is the experimentally determined dissociation energy (ref 23b).

cluster geometry I has the argon atom located above the center of a cyclohexane-like ring: dioxane$(Ar)_1$ has two such equivalent sites; ABCO$(Ar)_1$ and DABCO$(Ar)_1$ clusters have three such equivalent sites; and HMT$(AR)_1$ has four equivalent sites with this general structure. Geometry II for each cluster has the argon atom "coordinated to" the triangular face of the cyclohexane-like ring at the "foot" or "back" of the chair structure (HMT and dioxane) or the "bow" or "stern" of the boat structure (ABCO and DABCO). Geometry II has 2-fold degeneracy for dioxane$(Ar)_1$, 3-fold degeneracy for ABCO$(Ar)_1$, 6-fold degeneracy for DABCO$(Ar)_1$, and 12-fold degeneracy for HMT$(Ar)_1$. Geometry III is unique for ABCO$(Ar)_1$; it is similar to geometry II but the argon atom is bound to the tertiary carbon end of the ABCO molecule. Table 1 lists the binding energies for these cluster structures. These calculated values are in quite good agreement with the few experimental results that are reported.[23]

Figure 3 shows the mass-resolved excitation spectra (MRES) for dioxane-, ABCO-, DABCO-, and HMT$(Ar)_1$ plotted with respect to the appropriate bare molecule origin. The dioxane$(Ar)_1$ spectrum is a (2 + 1)-MRES but all others are taken as (1 + 1)-MRES.

The dioxane$(Ar)_1$ spectrum presents two features (60 cm^{-1} I, and 159 cm^{-1} II) which can be assigned as origins of two cluster geometries (I and II in Figure 2). The ABCO$(Ar)_1$ spectrum has three assignable origin features (I, II, and III) shifted from the bare molecule ABCO origin by 47, 245, and −28 cm^{-1}, respectively. The DABCO$(Ar)_1$ spectrum has two assignable origin features (I at 104 cm^{-1} and II 290 cm^{-1}). These correspond to the appropriate cluster structures depicted in Figure 2. Only one geometry is observed and assigned for HMT$(Ar)_1$, shifted 51 cm^{-1} to the blue of the HMT bare molecule origin. These transition shifts are summarized in Table 1.

The above transition energy blue shifts for the cluster Rydberg transitions demonstrate that the cluster binding energy in the Rydberg state is smaller than in the ground state. This results from an "exchange repulsion effect" or Pauli exclusion principle interaction for the Rydberg state. This interaction arises because the two species are held together by a van der Waals dispersion interaction at a roughly comparable distance in the two electronic states and the closed shells of the argon atom repel

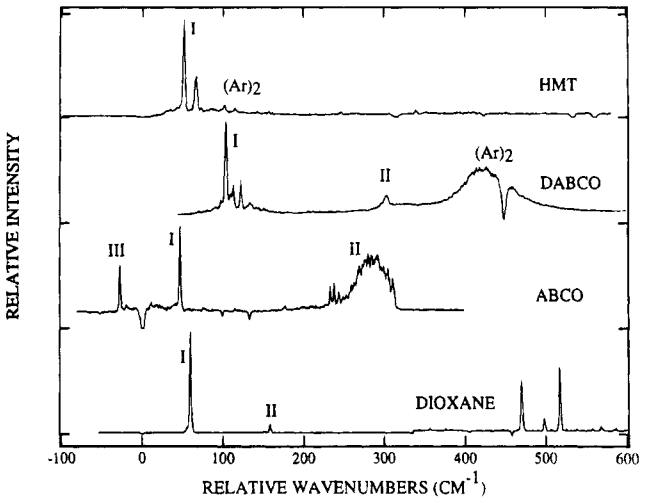

Figure 3. The MRES of dioxane$(Ar)_1$, ABCO$(Ar)_1$, DABCO$(Ar)_1$, and HMT$(Ar)_1$. The spectrum of dioxane$(Ar)_1$ is obtained via a (2 + 1) resonance-enhanced multiphoton ionization technique; the rest of spectra are obtained via a (1 + 1) resonance-enhanced multiphoton ionization technique. I, II, and III are assigned as O_0^0 transitions of the three geometries displayed in Figure 2. The designation $(Ar)_2$ indicates a feature from the dissociation of a solute-$(Ar)_2$ cluster appearing in the solute$(Ar)_1$ cluster mass channel. The bare molecule origins are 50 663 cm^{-1} for dioxane, 39 101 cm^{-1} for ABCO, 35 786 cm^{-1} for DABCO, and 42 141 cm^{-1} for HMT.

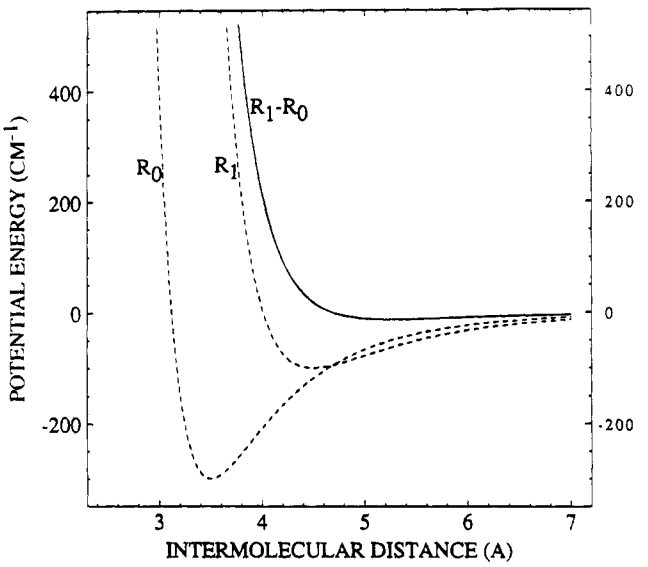

Figure 4. Intermolecular potential energy of ABCO$(Ar)_1$ cluster in the ground state and (2p3s) Rydberg state calculated by a Lennard-Jones 6−12 van der Waals interaction potential. The difference curve represents the Rydberg electron interaction with argon solvent (repulsion).

the 3s electron in its expanded, diffuse orbital (2p3s Rydberg state). The cluster in geometry II (Figures 2 and 3) has the larger shift because the solvent is closer to the major electron density (O or N atom) of the Rydberg orbital.

The red-shifted feature of ABCO$(Ar)_1$ is assigned to cluster geometry III (Figure 2) because this cluster structure has the argon atom at the furthest possible distance from the Rydberg state. At the tertiary carbon atom end of ABCO mostly dispersion forces must be present and since the excited state polarizability is in general larger than the ground state polarizability, the cluster is more tightly bound in the excited state than the ground state. Thus the cluster transition is lower in energy than the bare molecule transition. Some closed shell exchange repulsion could still exist at this solvation site which would reduce the full polarizability derived cluster red shift (as characterized for hydrocarbons and aromatic molecules[25]), but such a refined determination cannot be put forth at this time.

Cluster structure II for ABCO$(Ar)_1$ and DABCO-$(Ar)_1$ shows a very interesting property. As can be seen in Figure 3 both clusters show the feature marked II as broad and its line shape is truncated (the signal quickly falls to zero) on the high energy side. A concomitant rise in signal is observed in the respective bare molecule mass channel at this cutoff energy. The two signals, cluster and bare molecule, at this excitation energy are clearly coupled. We interpret this behavior as due to the cluster dissociating and generating a bare molecule. The blue shift in this instance, that is, the exchange repulsion interaction of the Rydberg state, is large enough to overcome the cluster dispersion interaction generated binding energy. The cluster thereby dissociates and the excited state potential well depth is ca. 100 cm^{-1}. The ground state binding energy estimated by potential energy calculation (Table 1) is consistent with this result.

The approximate solute/argon interaction potential for the Rydberg electronic distribution can be determined if the ground and excited state cluster binding energies are known. For ABCO$(Ar)_1$ the binding energy of the ground state is ca. 350 cm^{-1} (estimated from calculation, or cluster II blue shift and dissociation energy) and the excited state binding energy (estimated from cluster II line width) is ca. 100 cm^{-1}. Assuming a Lennard-Jones solute/solvent interaction potential function

$$V(r) = -A/R^6 + B/R^{12} \quad (1)$$

in which R is the distance between solute and solvent, one can model the ABCO/Ar interaction. The result of this estimate is given in Figure 4. If one assumes that the solute/solvent interaction for the electrons not undergoing excitation (promotion to the Rydberg 3s orbital) is roughly the same in the ground and excited states, the subtraction of the ground state potential from the excited state potential at each separation distance R represents the interaction of the electron in the Rydberg orbital with the solvent atom argon. One concludes based on Figure 4 that the interaction between an electron in the 3s Rydberg orbital and the argon solvent atom is repulsive. The repulsion decreases dramatically as the separation between the Rydberg molecule and the solvent increases; at $R \sim 4.5$ Å the interaction essentially vanishes. This crude modeling and simulated potential curve (Figure 4) are fairly consistent with the qualitative trends found for cluster transition shifts and cluster structure. Figure 4 also emphasizes that the cluster is much expanded in the Rydberg state: that is, the equilibrium solute/solvent separation is about 1 Å larger in the excited state than in the ground state.

As the number of solvent atoms increases for a cluster the transition shift behaves in a characteristic and predictable fashion. For example, DABCO-$(Ar)_{1,2,3}$ have origin features at blue shifts of 104, 206, 300 cm^{-1}, respectively. This shift additivity and regularity for each added solvent atom suggest that the argon atoms occupy equivalent sites about the solute in the cluster. Apparently the argon atoms occupy geometry I (Figure 2) sites in this instance and have little interaction with one another. This fact suggests that the Rydberg orbital extends to some degree throughout the molecule. Mixed site clusters can also be identified but in some cases, while sites occupation is readily assigned, simple blue shift additivity is not always found. Similar behavior has been characterized for $HMT(Ar)_n$, $n = 1, 2, 3$, for geometry I.

The cluster spectra for $DABCO(Ar)_{4,5}$ have also been observed. They are broad and quite blue shifted, but their spectra are not significantly blue shifted from one another. Presumably this result reflects a completed first solvent shell saturation of the solvent/Rydberg state interaction. One can also suggest that saturation of the cluster shift of the Rydberg transition at $n = 4$ and 5 implies that the two N atoms of DABCO contribute roughly equally to the Rydberg orbital, which must be nearly completely delocalized over the DABCO molecular framework.

2. Clusters with Other Rare Gas Atoms

The MRES of dioxane$(Kr)_1$ clusters[39] show similar but smaller blue-shifted transitions than do the dioxane$(Ar)_1$ clusters discussed above. The two detected geometries of dioxane$(Kr)_1$ have shifts of 22.6 and 107 cm^{-1}. The comparable Ar cluster shifts are 60 and 159 cm^{-1}. $DABCO(Kr)_1$ cluster blue shifts are 95 and 293 cm^{-1} for the two identified geometries (I and II), respectively. Larger DABCO/Kr clusters[30,42,43] also show additive shift behavior: geometry I clusters of $DABCO(Kr)_{2,3}$ have shifts of 185 and 281 cm^{-1}, respectively. $DABCO(Xe)_1$ spectra[43] are quite complex but the geometry I cluster can be assigned (first peak in the spectrum) with a 105 cm^{-1} blue shift.

One can rationalize these shift data as a balance between an increased dispersion interaction with increased polarizability of the solvent rare gas atom and an increased repulsive exclusion interaction as the solute/solvent pair are pulled closer together with respect to their van der Waals radii. Since the blue shift generally becomes smaller with increased solvent polarizability (i.e., Ar, Kr, Xe) one can speculate that the dispersion interaction, which causes the cluster transition to red shift, tends to increase more effectively as the solvent rare gas atom becomes heavier.

3. Dioxane-, ABCO-, DABCO-, and HMT/Saturated Hydrocarbon Clusters

The $(2p3s) \leftarrow (2p)^2$ Rydberg spectra of a number of hydrocarbon solvent clusters of dioxane,[39] ABCO, DABCO,[32c] and HMT[40] have been reported: these include dioxane/CH_4, dioxane/C_6H_{12}, HMT/CH_4, and ABCO- and $DABCO/C_mH_{2m+2}$ ($m = 1, ..., 7$). The CH_4 cluster spectra for these systems are very similar to those discussed above for Ar. The dioxane$(CH_4)_1$ spectrum shows an additional cluster feature (geometry) consistent with calculated structures for this system.[40] Of most interest here are the ABCO- and $DABCO/C_mH_{2m+2}$ clusters. As the chain length of the hydrocarbon increases in this series of solvents, a single cluster geometry predominates the cluster spectra. This is an unexpected result based on the calculation of the expected geometries and binding energies for these clusters. Apparently the cooling of these clusters is slow enough that the geometry of their global energy minimum can be exclusively populated. Figure 5 shows the transition energy blue shift for the observed ABCO cluster as a function of hydrocarbon chain length. As can be seen in this figure, the transition blue shift increases steeply as a function of *n*-alkane chain length from CH_4 to C_3H_8. The increase is much less steep from C_3H_8 to C_5H_{12}-, and is effectively saturated from C_5H_{12} to C_7H_{16} and for larger alkanes. This shift behavior can be interpreted or rationalized by assuming that each CH_2 group in an alkane chain contributes to the transition shift additively. For short-chain alkanes the CH_2 groups are close to the Rydberg orbital and thus the shift increases rapidly as the chain expands (e.g., CH_4 to C_3H_8). As more CH_2 groups are added, they are placed at further separation from the Rydberg orbital center and thus generate a small "solvent"-induced shift effect on the transition. At large enough separations, the additional CH_2 groups no longer have significant effect on the transition. This latter situation apparently occurs for the CH_3 groups of hexane which are roughly 5 Å from the Rydberg center nitrogen atom. This result supports the $ABCO(Ar)_1$ calculation of the extent of the Rydberg state interaction potential (Figure 4).

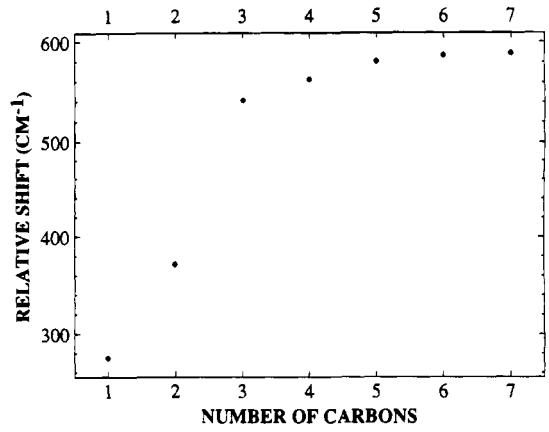

Figure 5. Plot of transition origin shifts for ABCO(*n*-alkane)$_1$ clusters with respect to the ABCO bare molecule origin.

4. Clusters with Other Solvents

Cluster transition blue shifts have been characterized for a number of other nonpolar solvents: dioxane$(SiH_4)_1$ and dioxane$(CF_4)_1$,[39] $DABCO(N_2)_1$,[32c] and $DABCO(C_2H_4)_1$. The point here is that the occurrence of a transition blue shift and its interpretation as arising from an exchange repulsion interaction for nonpolar solvents is quite general; it extends well beyond saturated hydrocarbons and rare gases.

B. Attractive Dipole/Induced Dipole Interaction

The Rydberg electron orbital is diffuse and thus highly polarizable. Therefore, the dipole/induced dipole interaction has the potential to be quite large if the solvent molecule in the cluster has a dipole moment. The dipole/induced dipole interaction is attractive and can thereby contribute to the overall stabilization of the cluster in the Rydberg state. In the presence of this interaction, one could expect polar solvent molecules to induce a cluster Rydberg transition red shift. A classical treatment of the dipole/induced dipole interaction can be expressed as[45]

$$V_{did} = -128\mu^2 \qquad (2)$$

in which μ is the dipole moment of the solvent molecule in debye. The constant term in this equation arises from a 100 Å^3 polarizability for the Rydberg electronic state and a center to center solute solvent distance of 5 Å. The Rydberg transition in a cluster of this nature could readily experience a red shift of a few hundred centimeters^{-1}. Since in this classical picture all interaction "types" are additive, this red shift would be expected to contribute to the total shift in addition to other shift mechanisms active for a particular solute/solvent pair. The presence of a dipole/induced dipole interaction for a Rydberg state is best demonstrated by the transition energy shift for the DABCO$(CH_3SCH_3)_1$ cluster (2p3s) ← $(2p)^2$ transition compared to that for the DABCO$(CH_3CH_2CH_3)_1$ cluster.[32c] The hydrocarbon solvent generates a cluster transition shift of 267 cm^{-1} while the thioether generates a cluster transition shift of 72 cm^{-1}. The reduced blue shift for the DABCO$(CH_3SCH_3)_1$ cluster transition can be understood if the exchange repulsion shift (hydrocarbon cluster) and the dipole/induced dipole shift are simply additive, opposite in sign, and apply only to the Rydberg state. The V_{did} term of eq 2 for μ = 1.5 D (CH_3SCH_3)[44] is ca. 200 cm^{-1} and thus a total shift for the thioether cluster of ca. 70 cm^{-1} is not unreasonable.

C. Attractive Electron Transfer Interaction

In addition to small spectroscopic red shifts and large blue shifts for cluster Rydberg transitions, one also observes some clusters with extremely large red shifted (2p3s) ← $(2p)^2$ Rydberg transitions. These species include DABCO clustered with amines, ether, and aromatic solvents. In some instances the red shifts approach 700 cm^{-1}.[30] More surprising than the size of the shifts, is that the shifts do not apparently correlate with classical electrical properties of the solvent molecules (see Table 2 for a few examples). To account for this behavior we have suggested that the electron in the 3s Rydberg orbital is delocalized into the available, similar, and equienergy virtual orbitals of the solvent molecules. This delocalization or electron transfer generates a strong attractive interaction between the (2p3s) excited DABCO molecule and the solvent molecule. If the solvent 3s Rydberg orbital is not close in energy to the DABCO 3s orbital this interaction is not very important. This interaction, and its concomitant red-shifted cluster (2p3s) ← $(2p)^2$ Rydberg transition, has been observed for a number of clusters (see Table 2). Such examples include HMT$(CH_3OCH_3)_1$ and HMT$(NH_3)_1$, for which the cluster red shifts are over 600 cm^{-1}, and the dioxane dimer, ABCO$(CH_3OCH_3)_1$ and ABCO$(NH_3)_1$.

Table 2. Transition Origin Shift of the Major Cluster Geometry of DABCO(Solvent)$_1$, Solvent Dipole Moment, Polarizability, and the Calculated Maximum Dipole/Induced Dipole Interaction Energy from Eq 2 in the Text

solvent molecule	transition origin shift (cm^{-1})	dipole moment[a] (D)	dipole/induced dipole interaction energy (cm^{-1})	solvent polarizability (Å^3)[a]
Ar	105	0	0	1.7
Kr	96	0	0	2.5
N_2	269	0	0	1.7
CH_4	149	0	0	2.6
C_2H_4	197	0	0	4.2
$CH_3CH_2CH_3$	267	0	0	6.3
cyclohexane	344	0	0	11.0
methylcyclohexane	358	–	–	–
DABCO	−541	0	0	–
TEA	−422	0.66	−491	13.1
ABCO	−685	1.2[b]	−184	–
NH_3	−136	1.47	−243	2.3
dioxane	−186	0	0	10.0
CH_3OCH_3	−455	1.3	−216	5.2
THP	−553	1.67[b]	−357	–
benzene	−334	0	0	10.3
toluene	−364	0.36	−166	12.3
CH_3SCH_3	72	1.5	−288	7.4
CH_3CN	−586	3.92	−1967	4.4

[a] Reference 44. [b] MOPAC 6(AM1) calculation.

This interaction and shift mechanism, once identified, can be found to be quite common for Rydberg states. One can attribute the large excited state binding energies of rare gas dimer (Xe_2, Ar_2) to such electron transfer. The Xe transition energy $(5p^56s^1)$ ← $(5p)^6$ is red shifted by nearly 5000 cm^{-1} (68 027 to 63 131 cm^{-1})[46] as the pressure of Xe gas increases from 1.3×10^{-3} to 50 atm in a static gas cell. We attribute this to an electron-transfer interaction between $(5p^56s^1)$Xe and the comparable virtual orbital configuration of surrounding $(5p)^6$Xe atoms. Additionally, Ar_2 is bound by 93 cm^{-1} in the ground state $(3p)^6$ configuration but the excited Ar $(3p^54s^1)$ is bound by ca. 5000 cm^{-1}.[46] The large excited state binding energy is due to an electron transfer between the Rydberg state atom and its comparable virtual state of the ground state atom. This mechanism seems to be characteristic of Rydberg states in general.

IV. Rydberg State Relaxation Dynamics and Reactions

One of the central characteristics of Rydberg electronic states is that the electron in the Rydberg orbital is not tightly bound to the molecular core. For a highly excited Rydberg state, the electron can be transferred to the environment, creating radical ion pairs. The general idea has been given practical realization for threshold ionization[26] and zero kinetic energy photoelectron spectroscopy (ZEKE, etc.).[27,28] Recently progress has been reported on the study of energy relaxation dynamics and reactions of the

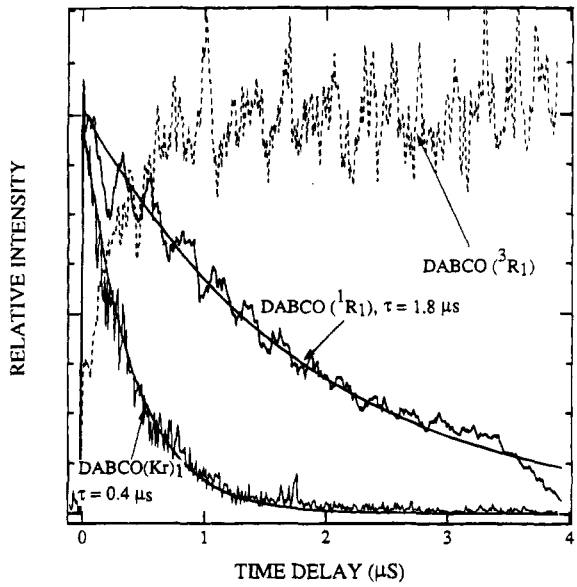

Figure 6. Pump/probe ionization lifetime decay of the DABCO singlet ($^1R_1$) state, triplet ($^3R_1$) state, and DABCO-(Kr)$_1$ ($^1R_1$) state. The solid smooth curves represent a fit of the experimental curve to a single exponential function. The abrupt decrease of the signal after 3.5 μs is due to the instrumental detection limit. The triplet state is generated from the DABCO(Kr)$_1$ Rydberg state dissociation. The DABCO(Kr)$_1$ cluster has geometry II.

(2p3s) lowest Rydberg state of many clusters. We will discuss these studies and results in the following paragraphs.

A. Intersystem Crossing[47]

An electron in a Rydberg orbital is poorly correlated to the electron in the valence shell of the core; this leads to a small energy difference between the singlet ($^1R_1$) and triplet ($^3R_1$) Rydberg states. Thus intersystem crossing can be readily induced or enhanced by the solvent molecule in a cluster. Cluster formation enhances the density of receiving states for intersystem crossing, and symmetry reduction and matrix element enhancement increase the spin–orbit coupling interaction in the cluster.

Intersystem crossing has been observed directly in DABCO/rare gas and saturated hydrocarbon clusters through pump/probe ionization experiments. For DABCO(Kr)$_1$ clusters, the decay of the $^1R_1$ state is much faster than for the bare DABCO molecule. Figure 6 shows this behavior for the geometry I and II clusters. As the DABCO(Kr)$_1$ cluster $^1R_1$ state decays, the DABCO bare molecule signal increases with the same time constant,[30] as shown in Figure 6 for cluster geometry II. The threshold ionization energy required to observe this newly created DABCO molecule is 550 cm^{-1} higher than that required for the $^1R_1$ excited bare molecule (Figure 7). We conclude from this that the molecule is generated in the $^3R_1$ state through the process:

$$\text{DABCO(Kr)}_1 \xrightarrow{h\nu} \text{DABCO(Kr)}_1\ ^1R_1 \rightarrow$$
$$\text{DABCO(Kr)}_1\ ^3R_1 \xrightarrow[\text{VP}]{\text{IVR}} \text{DABCO}\ ^3R_1 + \text{Kr}$$

The $^1R_1$ and $^3R_1$ states are separated by ca. 550 cm^{-1}. The $^3R_1$ DABCO has a very long lifetime, probably

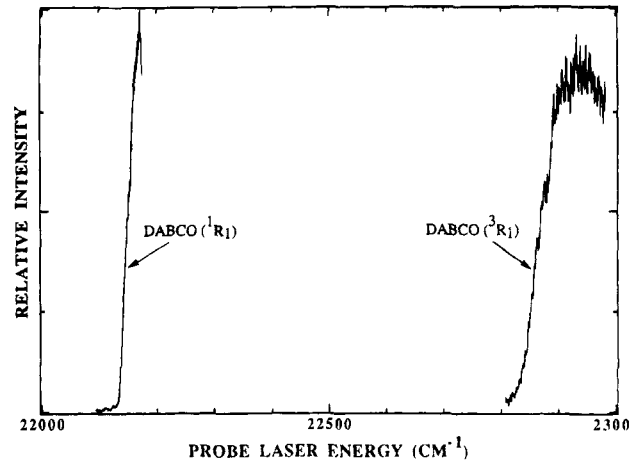

Figure 7. Photoionization threshold spectra of the excited singlet and triplet Rydberg states of DABCO. The singlet excited state ($^1R_1$) ionization curve is obtained by excitation of DABCO at its vibronic transition peak at 36 477 cm^{-1}. The triplet Rydberg state ($^3R_1$) ionization curve is obtained by excitation of the DABCO(Kr)$_1$ "geometry II" cluster transition at 36 075 cm^{-1}, while monitoring the DABCO ion mass channel with the ionization delayed 3 μs with respect to the excitation laser.

of the order of ms, as is clear from Figure 6. Kr is observed to enhance the intersystem crossing rate (cluster $^1R_1$ decay rate) much more than Ar or C_mH_{2m+2} solvent, as would be expected based on an external heavy atom effect mechanism. Additionally, the intersystem crossing rate is cluster geometry dependent: geometry II with the solvent near the nitrogen atom Rydberg center has a 5 to 6 times shorter lifetime than geometry I clusters.

HMT(Ar)$_1$ and HMT(CH$_4$)$_1$ also show similar behavior.[40] The rate for $^1R_1 \rightarrow {}^3R_x$ is even faster in this instance: the bare molecule ion signal rise time is less than 10 ns. In this system the singlet–triplet splitting is reduced to 255 cm^{-1}. Both the small $^1R_1$–^3R_x energy difference and the reduction of symmetry for HMT could contribute to this rapid decay. Unlike DABCO, however, this nascent triplet state does not live more than 25 ns. The bare HMT molecule is generated from the HMT(Ar)$_1$ cluster but not the HMT(CH$_4$)$_1$ cluster, which is apparently too tightly bound to dissociate with 255 cm^{-1} of vibrational energy. Nonetheless, even this cluster shows a 25 ns decay time for the nascent ^3R_x state. Most likely, lower triplets are generated by further internal conversion in both bare and clustered HMT.

B. Electron Transfer

An electron-transfer reaction for the (2p3s) Rydberg excited state of DABCO has been characterized for DABCO/amine, ether, and acetonitrile clusters.[30] The data upon which this assignment is based are cluster red shifts, binding energies, and time-dependent ionization behavior. An example of these latter results is presented in Figure 8. The MRES signal for these clusters has a rapid single exponential decay ($\tau \sim 0.2$ μs) to a constant value. This represents decay of cluster $^1R_1$ to a long-lived electron-transfer state which undergoes solvent reorganization and a concomitant increase in ionization cross section. The ionization threshold of the constant signal is 650 cm^{-1}

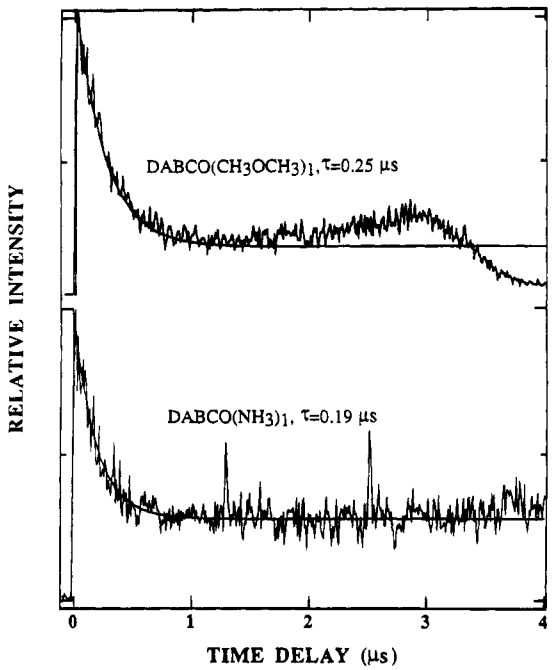

Figure 8. Decays of DABCO$(NH_3)_1$ and DABCO$(CH_3OCH_3)_1$ cluster (2p3s) Rydberg state excited at the origin transition. The ionization energy is 22 222 cm^{-1}. The decays for other DABCO amine and ether clusters are all similar. Note that the decays end in a constant signal for each case. These curves have been fit to a single exponential function plus a constant. The constant signal is assigned as due to long-lived charge-transfer intermediate.

higher in energy than that of the bare molecule. These results are in agreement with a rough calculation for the position of the cluster charge-transfer state.[30]

C. Energy Transfer

DABCO/aromatic solvent clusters evidence a somewhat different time-dependent behavior. These solvents do not have equienergy available virtual orbitals for electron transfer but do have readily available lower energy (singlet and triplet) valence states. No intermediate triplet states of the solvated or bare DABCO molecule are found for these systems. A rapid decay of $^1R_1$ for the cluster is observed and the enhanced cluster decay is attributed to energy transfer from $^1R_1$ DABCO to the aromatic valence states[30] which cannot be ionized with the energies employed in these experiments.

V. Conclusions

The study of Rydberg states in clusters is just at its beginning. The behavior of cluster Rydberg states is apparently much different than that of cluster valence states. The Rydberg states are highly sensitive to their environments. Only 3s Rydberg states have been thus far studied in this manner and higher states may have directional properties and may be even more environmentally sensitive than the (2p3s) states studied thus far. Reactivity is expected to increase as the Rydberg state energy (n) increases: both ion- and radical-like behavior can be anticipated from Rydberg state photochemistry. Electron-transfer reactions are anticipated to be more facile for higher Rydberg states, as well.

Acknowledgments. This research has been supported by the NSF and U.S. Army Research Office.

References

(1) (a) Bernstein, E. R., Ed. *Atomic and Molecular Clusters*; Elsevier: New York, 1990. (b) Bernstein, E. R., Ed. *Reactions in Clusters*; Oxford: New York, 1994. (c) Scoles, C. G., Ed. *Atomic and Molecular Beam Methods*; Oxford: New York, 1988, 1992; Vols. I, II. (d) Halberstadt, N., Janda, K. C., Eds. *Dynamics of Polyatomic van der Waals Molecules*; Plenum: New York, 1990. (e) Lubman, D. M., Ed. *Lasers and Mass Spectrometry*; Oxford: New York, 1990.

(2) (a) Amirav, A.; Even, U.; Jortner, J. *J. Chem. Phys.* **1981**, *75*, 2489. (b) Levy, D. H. *Adv. Chem. Phys.* **1981**, *41* (Pt. 1), 323.

(3) Matsushita, Y.; Kajii, Y.; Obi, K. *J. Phys. Chem.* **1992**, *96*, 6566.

(4) Castella, M.; Tramer, A.; Piuzzi, F. *Chem. Phys. Lett.* **1986**, *129*, 105.

(5) Crim, F. F. *Annu. Rev. Phys. Chem.* **1984**, *35*, 657.

(6) (a) Wittig, C.; Sharpe, S.; Beaudet, R. A. *Acc. Chem. Res.* **1988**, *21*, 341. (b) Bohmer, E.; Shin, S. K.; Chen, Y.; Wittig, C. *J. Chem. Phys.* **1992**, *97*, 2536. (c) Ionov, S. I.; Brucker, G. A.; Jaques, C.; Valachovic, L.; Wittig, C. *J. Chem. Phys.* **1992**, *97*, 9486. (d) Davis, H. F.; Ionov, P. I.; Ionov, S. I.; Wittig, C. *Chem. Phys. Lett.* **1993**, *215*, 214. (e) Ionov, S. I.; Brucker, G. A.; Jaques, C.; Chen, Y.; Wittig, C. *J. Chem. Phys.* **1993**, *99*, 3420. (f) Ionov, S. I.; Brucker, G. A.; Jaques, C.; Valachovic, L.; Wittig, C. *J. Chem. Phys.* **1993**, *99*, 6553. (g) Böhmer, E.; Mikhaylichenko, K.; Wittig, C. *J. Chem. Phys.* **1993**, *99*, 6545.

(7) Bernstein, E. R.; Law, K.; Schauer, M. *J. Chem. Phys.* **1984**, *80*, 207.

(8) Johnson, K. E.; Wharton, L.; Levy, D. H. *J. Chem. Phys.* **1978**, *69*, 2719.

(9) (a) Nimlos, M. R.; Kelley, D. F.; Bernstein, E. R. *J. Phys. Chem.* **1989**, *93*, 643. (b) Hineman, M. F.; Bruker, G. A.; Kelley, D. F.; Bernstein, E. R. *J. Chem. Phys.* **1992**, *97*, 3341. (c) Bernstein, E. R. *J. Phys. Chem.* **1992**, *96*, 10105. (d) Hineman, M.; Bernstein, E. R.; Kelley, D. F. *J. Chem. Phys.* **1993**, *98*, 2516. (e) Hineman, M.; Kelley, D. F.; Bernstein, E. R. *J. Chem. Phys.* **1993**, *99*, 4533. (f) Hineman, M.; Kelley, D. F.; Bernstein, E. R. *J. Chem. Phys.* **1994**, *101*, in press. (g) Kim, S. K.; Li, S.; Bernstein, E. R. *J. Chem. Phys.* **1991**, *95*, 3119.

(10) (a) Outhouse, E. A.; Bickel, G. A.; Dremmer, D. R.; Wallace, S. C. *J. Chem. Phys.* **1991**, *95*, 6261. (b) Ramackers, J. J. F.; Langelaar, J.; Rettschnick, R. P. H. In *Picosecond Phenomena III*; Eisenthal, K., Hochstrasser, R. M., Kaiser, W., Laubereau A., Eds.; Springer: Berlin, 1982; p 264. (c) Heppener, M.; Kunst, A. G. M.; Bebelaar, D.; Rettschnick, R. P. H. *J. Chem. Phys.* **1985**, *83*, 5314. (d) Heppener, M.; Rettschnick, R. P. H. In *Structure and Dynamics of Weakly Bound Molecular Complexes*; Weber, A., Ed.; Reider: Dordtrecht, 1978; p 553. (e) Ramackers, J. J. F.; Krijnen, L. B.; Lips, H. J.; Langelaar, J.; Rettschnick, R. P. H. *Laser Chem.* **1983**, *2*, 125. (f) Ramackers, J. J. F.; van Dijk, H. K.; Langelaar, J.; Resttschnick, R. P. H. *Faraday Discuss. Chem. Soc.* **1983**, *75*, 183.

(11) Li, S.; Bernstein, E. R. *J. Chem. Phys.* **1992**, *97*, 7383 and references therein.

(12) (a) Robin, M. B. *Higher Excited States of Polyatomic Molecules*; Academic Press: New York, 1974. (b) Even, U.; Levine, R. D.; Bersohn, R. *J. Phys. Chem.* **1994**, *98*, 3472 and general references therein, especially for higher energy Rydberg states and ionization.

(13) Causley, G. C.; Russell, B. R. *J. Chem. Phys.* **1980**, *72*, 2623.

(14) (a) Turro, N. *Modern Molecular Photochemistry*; Benjamin: Menlo Park, 1978. (b) Levine, R. D.; Bernstein, R. *Molecular Reaction Dynamics and Chemical Reactivity*; Oxford: New York, 1987.

(15) (a) Shaw, R. W., Jr.; Adams, G. F. *Diagnostics for Propellane Ignition*; Aberdeen: MD, 1984. (b) Olah, G. A.; Squire, D. R. *Chemistry of Energetic Materials*; Academic: New York, 1991.

(16) Herzberg, G. *Electronic Spectra and Electronic Structure of Polyatomic Molecules*; Van Nostrand: New York, 1966.

(17) Markovich, G.; Cheshnovsky, O. *J. Phys. Chem.* **1994**, *98*, 3550. Also see refs 1 and 3 and references therein.

(18) (a) Vaida, V. *Acc. Chem. Res.* **1986**, *19*, 114. (b) Donaldson, D. J.; Vaida, V.; Naaman, R. *J. Chem. Phys.* **1987**, *87*, 2522.

(19) Lie, S. H.; Fujimura, Y.; Neusser, H. J.; Schlag, E. W. *Multiphoton Spectroscopy of Molecules*; Academic: New York, 1984.

(20) (a) Nascimento, M. A. C. *Chem. Phys.* **1983**, *74*, 51. (b) McClain, W. M.; Harris, R. A. *Excited States*; Lim, E. C., Ed.; Academic Press: New York, 1977; Vol. 3.

(21) (a) Rizzo, T. R.; Park, Y. D.; Peteanu, L.; Levy, D. H. *J. Chem. Phys.* **1985**, *83*, 4819. (b) Rizzo, T. R.; Levy, D. H. In *Dynamics of Polyatomic van der Waals Molecules*; Halberstadt, N., Janda, K. C., Eds. Plenum: New York, 1990; p 402.

(22) Lipert, R. J.; Colson, S. D. *J. Phys. Chem.* **1989**, *93*, 135; 3894; *J. Chem. Phys.* **1988**, *89*, 4579; *Chem. Phys. Lett.* **1989**, *161*, 303.

(23) (a) Shang, Q. Y.; Bernstein, E. R. *J. Chem. Phys.* **1992**, *97*, 60. (b) Shang, Q. Y.; Moreno, P. O.; Li, S.; Bernstein, E. R. *J. Chem. Phys.* **1993**, *98*, 1876.
(24) Li, S., Bernstein, E. R. *J. Chem. Phys.* **1992**, *97*, 7383.
(25) (a) Smalley, R. E. In *Atomic and Molecular Clusters*; Bernstein, E. R., Ed.; Elsevier: New York, 1990; p 1. (b) Keese, R. G.; Castleman, W. A., Jr. In *Atomic and Molecular Clusters*; Bernstein, E. R., Ed.; Elsevier: New York, 1990; p 507. (c) Bernstein, E. R. In *Atomic and Molecular Clusters*; Bernstein, C. R., Ed.; Elsevier: New York, 1990; p 551. (d) Kager, J. W.; Wallace, S. C. In *Lasers and Mass Spectrometry*; Lubman, D. M.; Ed.; Oxford: New York, 1990; p 423.
(26) (a) Im, H. S.; Bernstein, E. R. *J. Chem. Phys.* **1991**, *95*, 6326. (b) Hager, J.; Wallace, S. C. *J. Chem. Phys.* **1986**, *84*, 6771. (c) Rohlfing, E. A.; Cox, D. M.; Kaldor, A.; Johnson, K. H. *J. Chem. Phys.* **1984**, *81*, 3846.
(27) (a) Müller-Dethlefs, K.; Schlag, E. W. *Annu. Rev. Phys. Chem.* **1991**, *42*, 109. (b) Grant, E. R.; White, M. G. *Nature* **1991**, *354*, 249.
(28) (a) Zhu, L.; Johnson, P. *J. Chem. Phys.* **1991**, *94*, 5769. (b) Hillenbrand, S.; Zhu, L.; Johnson, P. *J. Chem. Phys.* **1991**, *95*, 2237. (c) Takazawa, K.; Fujii, M.; Ebata, T.; Ito, M. *Chem. Phys. Lett.* **1992**, *189*, 592. (d) Krause, H.; Neusser, H. J. *J. Chem. Phys.* **1992**, *97*, 5923. (e) Jouvet, C.; Dedonder-Lardeux, C.; Martrenchard-Barra, S.; Solgadi, D. *Chem. Phys. Lett.* **1992**, *198*, 419.
(29) Lipert, R. J.; Colson, S. D.; Sur, A. *J. Phys. Chem.* **1988**, *92*, 183.
(30) Shang, Q. Y.; Moreno, P. O.; Bernstein, E. R. *J. Am. Chem. Soc.* **1994**, *116*, 302; 311.
(31) (a) Hineman, M. F.; Bruker, G. A.; Kelley, D. F.; Bernstein, E. R. *J. Chem. Phys.* **1992**, *97*, 3341. (b) Syage, J. A.; Steadman, J. *J. Chem. Phys.* **1991**, *95*, 2497; 10326; **1990**, *92*, 4630. (c) Steadman, J.; Syage, J. A. *J. Am. Chem. Soc.* **1991**, *113*, 6786; *J. Phys. Chem.* **1992**, *96*, 9606. (d) Syage, J. A. *J. Phys. Chem.* **1993**, *97*, 12523. (e) Breen, J. J.; Peng, L. W.; Willberg, D. M.; Heikal, A.; Cong, P.; Zewail, A. H. *J. Chem. Phys.* **1990**, *92*, 805. (f) Cheshnowsky, O.; Leutwyler, S. *Chem. Phys. Lett.* **1985**, *121*, 1; *J. Chem. Phys.* **1988**, *88*, 4127. (g) Knochenmuss, R.; Holtom, G. R.; Ray, D. *Chem. Phys. Lett.* **1993**, *215*, 188. (h) Knochenmuss, R.; Cheshnowsky, O.; Leutwyler, S. *Chem. Phys. Lett.* **1988**, *144*, 317. (i) Droz, T.; Knochenmuss, R.; Leutwyler, S. *J. Chem. Phys.* **1990**, *93*, 4520.
(32) (a) Nowak, R.; Menapace, J. A.; Bernstein, E. R. *J. Chem. Phys.* **1988**, *89*, 1309. (b) Menapace, J. A.; Bernstein, E. R. *J. Phys. Chem.* **1987**, *91*, 2533; 2843. (c) Shang, Q. Y.; Moreno, P. O.; Dion, C.; Bernstein, E. R. *J. Chem. Phys.* **1993**, *98*, 6769. (d) Disselkamp, R.; Bernstein, E. R. *J. Chem. Phys.* **1993**, *98*, 4339.
(33) (a) Klemperer, W.; Yaron, D.; Nelson, D. D. *Faraday Discuss. Chem. Soc.* **1988**, *86*, 261. (b) Nelson, D. O.; Fraser, G. T.; Klemperer, W. *Science* **1987**, *238*, 1670; Klemperer, W. *Science* **1992**, *257*, 887. (c) Weber, A., Ed. *Structure and Dynamics of Weakly Bound Molecular Complexes*; Reidel: Dordrecht, 1987. (d) Nesbitt, D. J.; Naaman, R. *J. Chem. Phys.* **1989**, *91*, 3801. (e) Nesbitt, D. J. *Chem. Rev.* **1988**, *88*, 843. (f) Miller, R. E. *Science* **1988**, *240*, 447.
(34) Kung, C. Y.; Miller, T. A.; Kennedy, R. A. *Phil. Trans. R. Soc. (Lond.) A* **1988**, *324*, 223.
(35) Mizukarni, Y.; Nakatsuji, H. *J. Chem. Phys.* **1990**, *92*, 6084.
(36) (a) Hobza, P.; Selzle, H. L.; Schlag, E. W. *J. Chem. Phys.* **1990**, *93*, 5893; *J. Phys. Chem.* **1993**, *97*, 3937; *J. Chem. Phys.* **1991**, *95*, 391; *J. Am. Chem. Soc.* **1994**, *116*, 3500 and references to earlier work therein. (b) Hobza, P.; Bludsky, O.; Selzle, H. L.; Schlag, E. W. *J. Chem. Phys.* **1993**, *98*, 6223; **1992**, *97*, 335.
(37) (a) Wanna, J.; Menapace, J. A.; Bernstein, E. R. *J. Chem. Phys.* **1986**, *85*, 1795. (b) Augspurger, J. D.; Dyktra, C. E.; Zwier, T. S. *J. Phys. Chem.* **1992**, *96*, 7252. (c) van der Avoird, C. A. *J. Chem. Phys.* **1993**, *98*, 5327. (d) Schauer, M.; Bernstein, E. R. *J. Chem. Phys.* **1985**, *82*, 3722. (e) Ondrechen, M. J.; Berkovitch-Yellin, A.; Jortner, J. *J. Am. Chem. Soc.* **1981**, *103*, 6586.
(38) (a) Robin, M. B.; Kuebler, N. A. *J. Mol. Spectrosc.* **1970**, *33*, 274. (b) Miladi, M.; Falher, J.-P. LE; Roncin, J.-Y.; Damany, H. *J. Mol. Spectrosc.* **1975**, *55*, 81.
(39) Moreno, P. O.; Shang, Q. Y.; Bernstein, E. R. *J. Chem. Phys.* **1992**, *97*, 2869.
(40) Shang, Q. Y.; Dion, C.; Bernstein, E. R. *J. Chem. Phys.* **1994**, *101*, in press.
(41) Nemethy, G.; Pottle, M. S.; Scheraga, H. A. *J. Phys. Chem.* **1983**, *87*, 1883 and ref 1.
(42) Bahatt, D.; Even, U.; Gedanken, A. *J. Phys. Chem.* **1993**, *97*, 7189.
(43) van der Hoek, G.; Consalvo, D.; Parker, D. H.; Reuss, J. Private communication.
(44) Lide, D. R. *Handbook of Chemistry and Physics*, 71st ed.; CRC Press: Boca Raton, 1990–1991.
(45) McLennan, J. C.; Turnbull, R. *Proc. R. Soc. (Lond.), Ser. A* **1930**, *129*, 266.
(46) (a) Herman, P. R.; LaRocque, P. E.; Stoicheff, B. P. *J. Chem. Phys.* **1988**, *89*, 4535.
(47) See for example: (a) Zahlan, A. B.; Ed. *The Triplet State*; Cambridge: New York, 1967. (b) El-Sayed, M. A. In *Excited States*; Lim, E. C.; Academic: New York, 1974; Vol. II, p 35.